Biomacromolecules

Article

Superior Performance of Polyurethane Based on Natural Melanin Nanoparticles

Yang Wang, Ting Li, Xuefei Wang, Piming Ma, Huiyu Bai, Weifu Dong, Yi Xie, and Mingqing Chen

Biomacromolecules, **Just Accepted Manuscript** • DOI: 10.1021/acs.biomac.6b01298 • Publication Date (Web): 17 Oct 2016

Superior Performance of Polyurethane Based on Natural Melanin Nanoparticles

Yang Wang, Ting Li, Xuefei Wang, Piming Ma, Huiyu Bai, Weifu Dong*, Yi Xie, Mingqing Chen*

*E-mail: wfdong@jiangnan.edu.cn, mqchen@jiangnan.edu.cn.

Tel.: +86-510-8532-6290. Fax: +86-510-8591-7763.

The Key Laboratory of Food Colloids and Biotechnology, Ministry of Education, School of Chemical and Material Engineering, Jiangnan University, 1800 Lihu Road, Wuxi 214122, China

Keywords: Polyurethane; Melanin; Phase separation; Mechanical properties

ABSTRACT: Melanin, a kind of well-known multifunctional biomacromolecules that are widely distributed in natural sources. In this work, Polyurethane (PU)/melanin nanocomposites with enhanced tensile strength and toughness were successfully fabricated *via* in situ polymerization. It was found that the tensile strength (σ), elongation-at-break (ε_{max}) and toughness (W) were improved from 5.6 MPa, 770% and 33 MJ/m^3 for PU to 51.5 MPa, 1880% and 413 MJ/m^3 for PU/melanin (2 wt %) nanocomposite, respectively. Micromorphology indicated that individualized melanin nanoparticles were specifically linked to the hard domains of PU chains and fine dispersed in matrix. FTIR, DSC and AFM results suggested melanin

induced an improvement in degree of phase separation, which resulted in remarkable enhancements in mechanical properties of PU. However, with further increasing content of melanin, a relatively large-scale phase separation was formed and led to a decrease in mechanical properties of PU. In addition, interactions between melanin and hard segments of PU were increased, leading to a higher T_{gHS}. Moreover, the dynamic mechanical properties and rheological behavior of PU/melanin nanocomposites were further investigated.

Introduction

Polyurethane (PU) is an important polymer material with a liner block copolymer structure with alternating amorphous soft and semicrystalline hard segments, which is widely demanded in many fields such as coatings, foams, and elastomers owing to its outstanding biocompatible, flexibility and easy processibility.[1-3] The hard segment consists of diisocyanate and a low molecular weight chain extender, while the soft segment is composed of polyester or polyether polyol.[4] The thermodynamic incompatibility between the soft and hard segments leads to the formation of phase separation.[5, 6] The hard domains are considered as the "physical cross-linkers" and reinforcing fillers in PU. The degree of phase separations, which are dependent on many factors, such as molecular structure, the molar mass distribution of composition, and the interaction between each segments, makes a great difference in the properties of PU.[7, 8] The stiffness and strength of PU are increased with hard segments loading while the extensibility is increased with soft segments loading.[9-11] Obviously, it is challenging to improve the strength of PU and simultaneously keep its stronger toughness, or scilicet an enhancement in one usually causes a sacrifice in the other. In consequence, it is imperative to exploit a simple process to design PU with excellent properties by controlling its phase separations.[12]

Polymer nanocomposites have attracted a range of interest due to their extraordinary properties.[13, 14] A serials of nanofillers, including of silica, clay, carbon nanotubes (CNTs), hydroxyapatite and graphene oxide (GO) have been extensively used to modify PU.[3-8] On basis of clay, PU nanocomposites were prepared *via* solvent exchange processing.[15] It was found that the morphological changed over a range of large phase separation was caused by introduction of the clay platelets, showing more interconnected hard phases that led to significant enhancement of mechanical properties. PU containing polyhedral oligomeric silsesquioxanes (POSS) as side chain to the hard segments showed extensive phase separation.[16] However, the poor adhesion hard segments often decrease the toughness of PU. Moreover, GO can reinforce PU because of its unique properties.[17, 18] However, for carbon-based nanomaterials, the weak interfacial interaction between GO and PU was one of the main challenges in application. Tremendous efforts had also been exploited to functionalized GO sheets to improve their interfacial interactions, which made the synthesis processes more complicated.[17, 19] Recently, PU/cellulose nanocrystals (CNCs)[20] or PU/microfibrillate cellulose (MFC)[21] nanocomposites with improved strength and extensibility were fabricated. During the preparation, the prepolymers terminated with isocyanate were grafted onto the surface of cellulose, and the covalent bonds induced phase separation. As known to all, MFC or CNCs were obtained from wood fiber cell wall by endoglucanases or acid hydrolysis[22] in combination with multipass high-pressure homogenization[23], which meant the applications were more difficult in large scale.

Melanin are well-known multifunctional biomacromolecules that are widely distributed in nature, and display antibacterial activity, photoprotection, and free radical scavenging activities.[24, 25] However, few exploitation of melanin to enhance polymer materials has been reported compared with other biomacromolecules such as nanocellulose,[26, 27] chitin[28] or

collagen.[29] The nanoparticle characteristics are usually considered as the most remarkable features of melanin. Normally, melanin isolated from the cuttlefish has been chosen as a standard due to their simple separation and high purity. Although the exact knowledge of its structure, especially at the molecular level, remains poorly documented, many reactive functional groups (–OH, –NH and –COOH) indeed exist in melanin.[30-32] Generally, particles with three or more reactive vertex groups act as comparatively massive, three-dimensional chemical cross-linkers. Thus, melanin may be an ideal nanobuilding block due to the versatility in reactive groups may possess. In our previous studies, strong and robust PVA nanocomposites were prepared with the addition of melanin nanoparticles. The dramatic enhancement in the mechanical properties of PVA were achieved by the strong hydrogen bonds interaction between melanin and PVA.[24, 25, 33]

According to these studies, in this work, PU/melanin nanocomposites were successfully prepared via in situ polymerization. It was shown that a significant improvement in strength and toughness of PU was achieved by loading a small amount of melanin. Furthermore, the effect of melanin on the microphase and macroscopic properties of PUs was investigated.

Experimental Section

Materials

N,*N*-Dimethylformamide (DMF, 99.8%), 4,4′-Diphenylmethane diisocyanate (MDI, 98%), and 1,4-butanediol (1,4-BD, 99%) were all purchased from Aladdin (Shanghai, China). Poly(tetramethylene glycol) (PTMG, average M_n=1000) was obtained from Aldrich. MDI was heated at 60 ℃ and pressure filtered in N_2 atmosphere. After that, pure MDI was achieved through recrystallization. DMF and 1,4-BD were dehydrated with the molecular sieves for 24 h

and freshly redistilled under vacuum. PTMG was used after 2 h of drying under vacuum at 110 ℃.

Extraction of Natural melanin

Ink sacs were prepared from of Sepia officinalis. Melanin nanoparticles were separated from the freshly dissected ink sac with centrifuging (18,000 rpm, 15 min). After several times of washing, a clean melanin nanoparticles dispersion was received. The excess water were removed under vacuum (50 ℃) for 24 h to obtain dry melanin nanoparticles.

Preparation of PU/melanin Nanocomposites

PU prepolymer was prepared *via* the reaction of MDI and PTMG in DMF solvent. The reaction took place at a temperature of 90 ℃, and under a dry N_2 for 2 h with mechanical stirring. Then the reaction was detected using ATR. The disappearance of hydroxyl peak indicated completion of step 1. Subsequently, the predetermined loading of melanin dispersed in DMF solvent was incorporated and stirred for another 1 h. Then 1,4-BD was added for reacting with the residual isocyanate groups (**Scheme 1**). After that, the products were casted on a Teflon dish, and drying at 80 ℃ for 24 h to receive the plaque. The plaque were dried for 24 h in vacuum oven at 80 ℃ to remove the residual DMF. The amount of reactive groups (–OH, –NH and –COOH) on melanin was 5.62 mmol/g as determined using titration to measure the residual –NCO of MDI after reacting with a given amount of melanin. PU nanocomposites including 0.5, 1, 2 and 5 wt % melanin were fabricated through changing the loading of melanin and 1,4-BD.

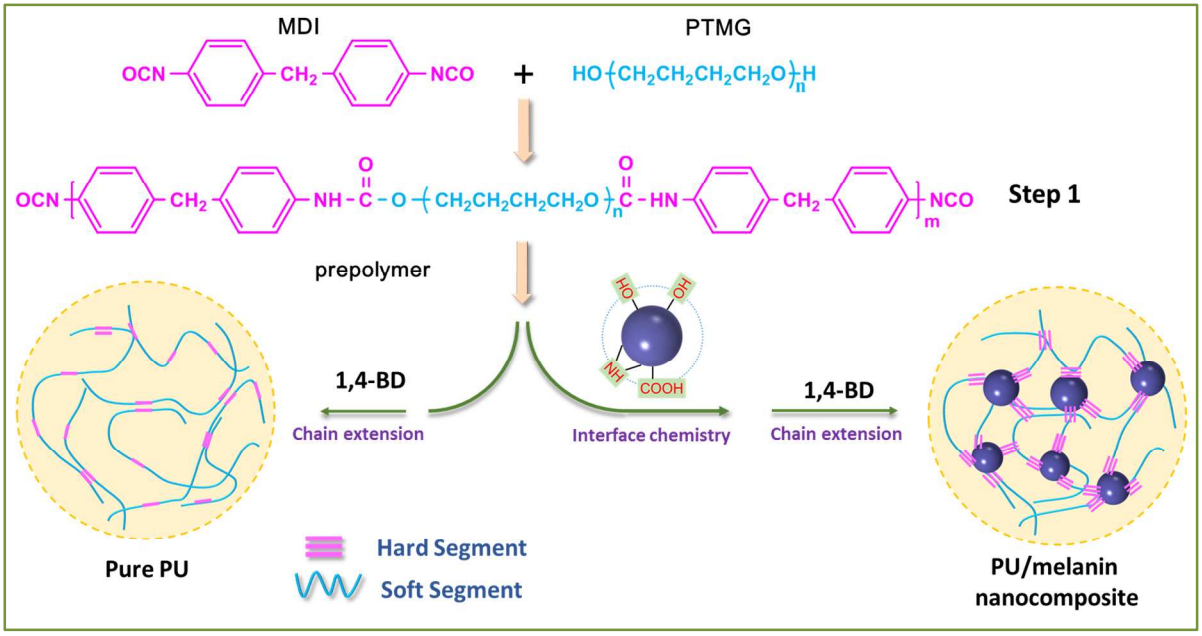

Scheme 1. Synthetic procedure to prepare PU and PU/melanin nanocomposites

Characterizations

The infrared spectra of sample were performed by the attenuated total reflection (ATR, Nicolet 6700).The spectra were recorded from 600 to 4000 cm^{-1} with resolution of 4 cm^{-1}.

To investigate the interactions between PU and melanin nanoparticles, Soxhlet extraction in which acetone as solvent was used to isolate melanin from the nanocomposites. The residue (melanin-PU nanohybrids) was dried under vacuum (50 ℃, 24 h). The atomic force microscope (MuLtimode 8, Bruker Nano, USA) was performed in a peak-force-error mode to characterize the morphology of melanin and melanin-PU nanohybrids. Furthermore, the AFM phase images of PU and PU/melanin films were obtained at ambient temperature. Tapping mode AFM was conducted via Nanosensors PPP-NCH AFM probes (spring constant 35 N/m). Tapping forces were in the range of 0.6.

The morphologies of melanin nanoparticles, melanin-PU nanohybrids and fracture surfaces of PU/melanin nanocomposites were observed with scanning electron microscopy (SEM Hitachi S4800). The ultrathin sections of samples were microtomed at -90 ℃ (70-100 nm in thickness). The morphology of PU/melanin nanocomposites were observed with TEM (Philips TECNAI 20).

Mechanical properties were performed on Instron 5967 teasting machine. A crosshead speed of 50 mm/min was applied. Five specimens of each sample were tested.

Dynamic Mechanical Analysis was operated on TA Instruments Q800 DMA. The specimens were cut into 15×5.3×0.5 mm^3 and measured with a heating rate of 3 ℃/min from -80 to 100 ℃ and the frequency was 1Hz.

The glass transition temperature for soft and hard segments (T_{gSS} and T_{gHS}, respectively) of PU and PU/melanin nanocomposites were assessed with a differential scanning calorimetry of DSC 8000 analyzer (PerkinElmer, USA). An empty aluminum crucible was used as reference. The samples were heated at a rate of 10 ℃/min over the range of -80 to 240 ℃ in N_2 atmosphere. T_{gSS} and T_{gHS} were chosen as the inflection point from the DSC curve.

Dynamic rheological analyses (DRA) were performed by using a DHR-2 rheometer (TA Instruments, USA). The experiment were carried on 25 mm diameter plate, with 1 mm in gap at 200 ℃. The tests were examined in a frequency-sweep mode with the frequency from 100 to 0.01 Hz in the linear viscoelastic range.

Results and discussion

FTIR

Figure 1 showed FTIR spectroscopy of PU, melanin and PU/melanin nanocomposites. For PU/melanin nanocomposites, the new absorption peak at about 1646 cm^{-1} was attributed to C=O, and another peak at about 1510 cm^{-1} was attributed to N–H and C–N.[21] These results indicated the reaction between –OH of melanin and –NCO was successfully performed. For all the spectra of PU and its nanocomposites, the peak observed at about 3300 cm^{-1} was ascribed to N-H stretching. In addition, the two peaks located at 1730 and 1708 cm^{-1}, according to free carbonyl and hydrogen-bonded carbonyl groups, and the peak intensity ratios of these two peaks revealed the degree of phase separation. The carbonyl hydrogen-bonding index (R) is calculated from equation $R= A_{1708}/A_{1730}$, and the degree of phase separation (DPS) is obtained by formula DPS= $R/(R+1)$.[34] It was clear that R increased with increasing melanin content (**Table 1**). All results suggested that melanin had a significant influence on the phase separation of PU.

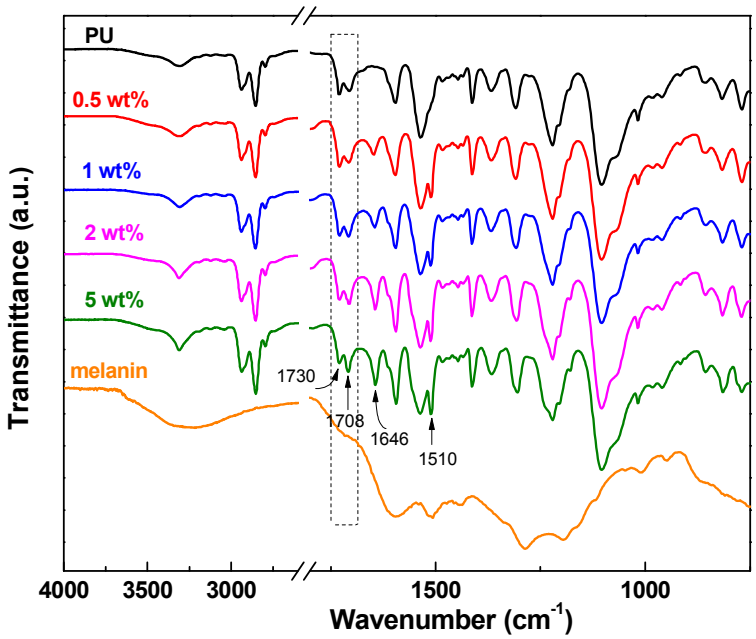

Figure 1. FTIR spectra of PU, melanin and PU/melanin nanocomposites.

Table 1 The carbonyl hydrogen bonding index (R) and the degree of phase separation (DPS) in PU/melanin nanocomposites.

	R (A_{1708}/A_{1730})[a]	DPS (%)
PU	0.65	39
0.5 wt %	1.29	56
1 wt %	1.77	64
2 wt %	2.36	70
5 wt %	2.84	74

[a] The carbonyl hydrogen bonding index obtained from A_{1708}/A_{1730} in the FTIR curve.

Mechanical properties

Stress-strain curves of nanocomposites were recorded. E_1 was the Young's modulus. E_2 and E_3 were calculated by the slope of the stress–strain curves, as schematized in **Figure 2**. Toughness can be calculated by equation (1), i.e.,

$$\mathrm{W} = \int_0^{\varepsilon_{max}} \sigma' \, d\varepsilon \qquad (1)$$

where the σ' and ε are the stress and strain, respectively. Tensile strength (σ), elongation-at-break (ε_{max}), Young's modulus (E_1) and toughness (W) of the PU were about 5.6±1.5 MPa, 770.2 ± 25.6%, 6.3 ± 0.6 MPa and 33.1 ± 5.6 MJ/m^3, respectively, which were in well accordance with the previous reports (as shown in **Table 2**).[20] With addition of only 0.5 wt % melanin, σ and ε_{max} were increased to 25.5±3.5 MPa and 2598.1 ± 56.1%, respectively. With further increasing content of melanin, σ, ε_{max} and E_1 of PU/melanin-2 wt % nanocomposite were enhanced to 51.5±1.6 MPa, 1881.7 ± 51.5% and 21.3 ± 1.5 MPa, respectively, which were much greater than these of PU. On the other hand, W of nanocomposite reached the

highest value of 484.1±36.6 MJ/m^3 with 1 wt % melanin, which was more than 15-fold higher than that of PU. Additionally, PU/melanin nanocomposites showed three regions in the stress-strain curves. Region (1) "quasi-linear elastic deformation region" emerged in at the initial stage. σ and ε_{max} were dominated by PU crystallinity, the content and ordering of hard segments; Region (2) "moderate-modulus region" governed by the deformation of soft domains and alignment of hard domains, and Region (3) "strain-hardening region" associated with the break-up of hard domains and unraveling of the entangled nanoparticles. The strong interaction allowed the nanocomposite to bear stronger force and shape greater deformation. With addition of 1, 2 wt % melanin, nanocomposites exhibited an obvious strain-hardening behavior, showing E_3 enhancements, not presented on PU. Strain-hardening suggested the strong cohesion force between hard segments. Generally, direct blending thermoplastic matrices and rigid fillers offers improvements in modulus and tensile stress at the expense of a sacrifice in extensibility. Surprisingly, a small amount of melanin enhanced the modulus and strength while at the same time dramatically improved the toughness of PU in this work.

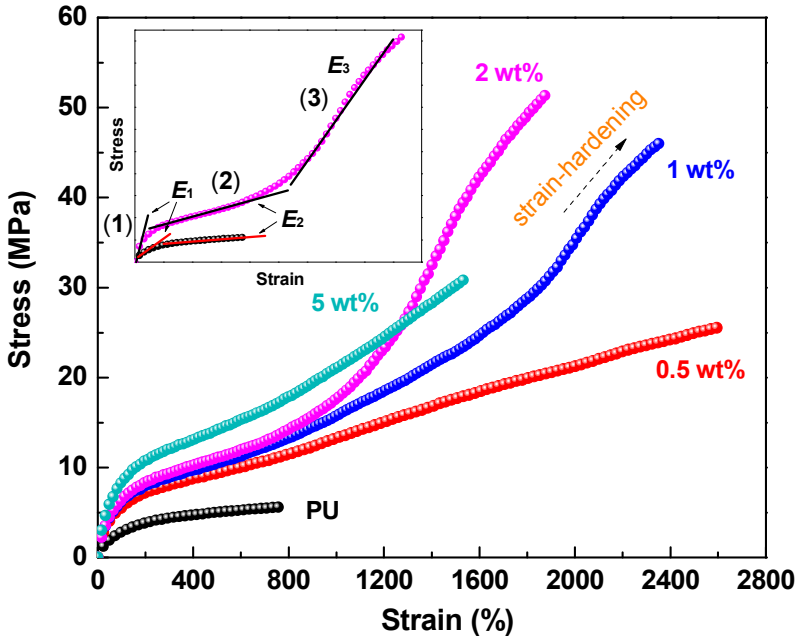

Figure 2. Tensile testing curves of PU and PU/melanin nanocomposites.

Table 2 Mechanical Properties of PU and PU/melanin Nanocomposites: Tensile strength (σ), Elongation-at-Break (ε_{max}), Young's Modulus (E_1), Modulus 2 (E_2), Modulus 3 (E_3) and Toughness (W).

sample	σ (MPa)	ε_{max} (%)	E_1 (MPa)	E_2 (MPa)	E_3 (MPa)	W (MJ/m^3)
PU	5.6±1.4	770.2±25.6	6.3±0.6	0.19±0.04	-	33.1±5.6
0.5 wt %	25.5±3.5	2598.1±94.3	17.5±1.2	0.66±0.02	0.89±0.08	406.6±25.5
1 wt %	46.1±2.4	2350.4±56.1	19.2±1.6	0.83±0.01	3.9±0.13	484.1±36.6
2 wt %	51.5±1.6	1881.7±51.5	21.3±1.5	0.91±0.02	5.5±0.20	413.2±27.9
5 wt %	31.2±1.2	1544.4±79.3	26.3±2.0	1.1±0.08	1.79±0.04	280.5±21.3

DSC analysis

As shown in **Figure 3,** the transition around -34.8 ℃ and 56.2 ℃ were corresponded to T_{gSS} and T_{gHS} of PU, respectively. With increased melanin content, T_{gSS} was decreased to -49.2 ℃, and T_{gHS} was increased to 97.2 ℃. T_g is often dependent on the flexibility of PU chain, the higher T_g, the more immovable chains. The relatively higher T_{gSS} was observed in PU, which was due to the fact that hard domains were more fine dispersed in PU and had more restriction on the soft segments mobility. Actually, a lower T_{gSS} is often taken to be indicative of a greater degree of phase separation in PU.[35] PU/melanin nanocomposites displayed lower T_{gSS}, indicating that the addition of melanin induced phase separation. On the other hand, with addition of melanin, strong interactions between melanin and hard segments was formed and brought about more hindrance to the hard segments movements, leading to higher T_{gHS} enhanced. In conclusion, a decrease of T_{gSS} for PU with melanin

suggested an enhancement for degree of phase separation, and the increase of T_{gHS} implied a stronger interaction in hard domains by introduction of melanin.

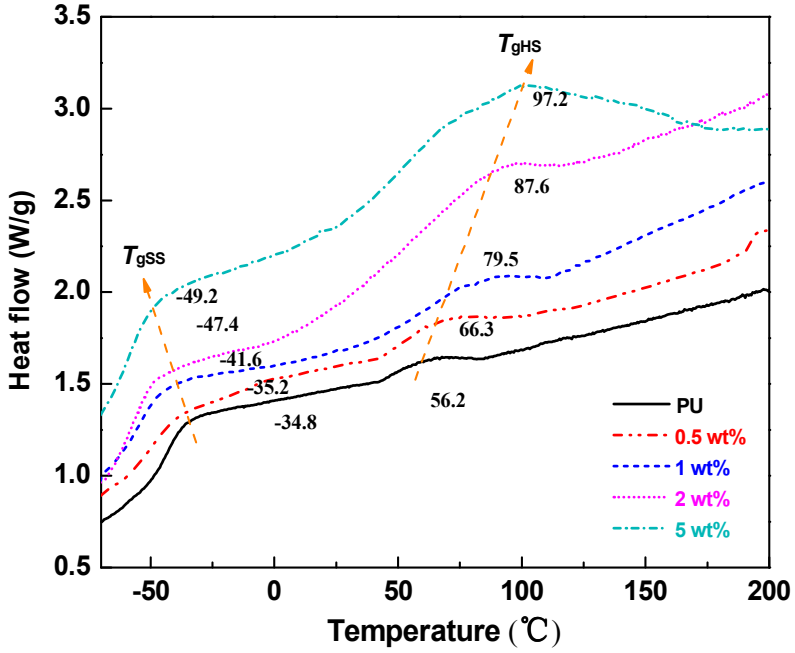

Figure 3. DSC curves of PU and PU/melanin nanocomposites.

Dynamic mechanical properties

The storage modulus of pure PU displayed a drastic reduction at its T_g, and maintained decreasing with an increase of temperature in the rubbery region (as shown in **Figure 4**). Interestingly, an excellent improvement in high temperature range was obtained when melanin was introduced into the PU matrix. With addition of 2 wt % melanin, the modulus of the nanocomposite was 600% and 830% better than that of pure PU at temperature of 20 and 60 ℃, which further confirmed that the introduction of melanin was able to enhance the

mechanical properties of PU. For pure PU, the tan δ at around -21.6 ℃ attributed to T_{gSS} of PU. However, T_{gSS} decreased with increasing melanin loading, as was shown in **Figure 4 (b)**.

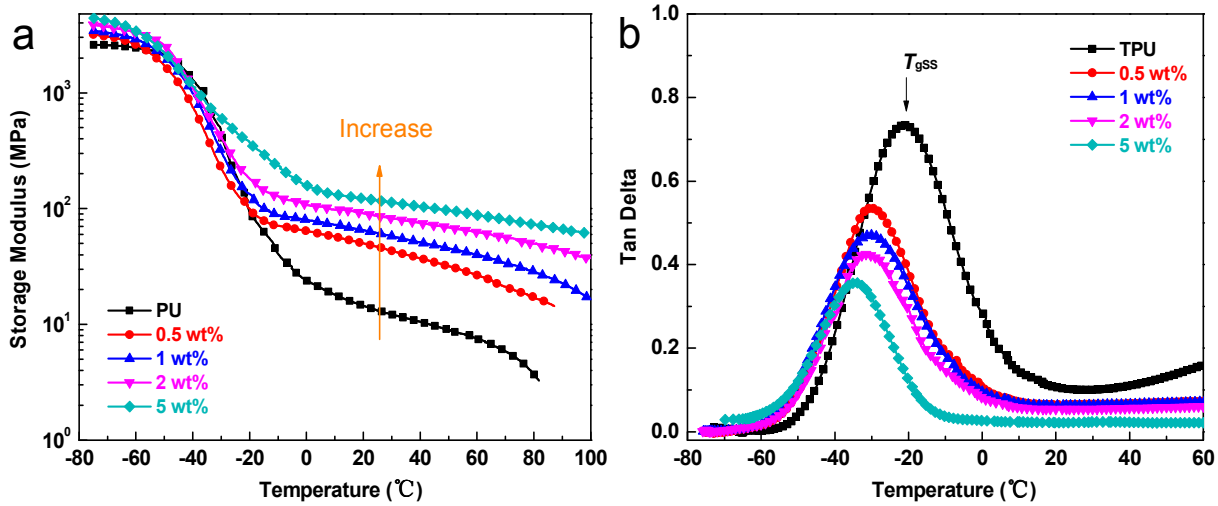

Figure 4. (a) Storage modulus and (b) tan δ of PU and PU/melanin nanocomposites.

Morphological Characterization

Typical scanning electron microscopy (SEM) image showed that melanin nanoparticles were sphere in shape, with diameters of approximately 150-200 nm (**Figure 5a**). Through a Soxhlet extraction process, the residues (melanin-PU nanohybrids) were obtained and SEM image was seen in **Figure 5b**. Compared with the original melanin nanoparticles, melanin-PU nanohybrids exhibited irregular sphere with some dots on the rough surface, which was owning to the depositing of PU on the melanin surface. These changes in surface morphology of melanin revealed successful grafted PU chains on the melanin surface. At the same time, melanin and melanin-PU nanohybrids were also evidenced by AFM images (**Figure 5c**, **d** and **e**).

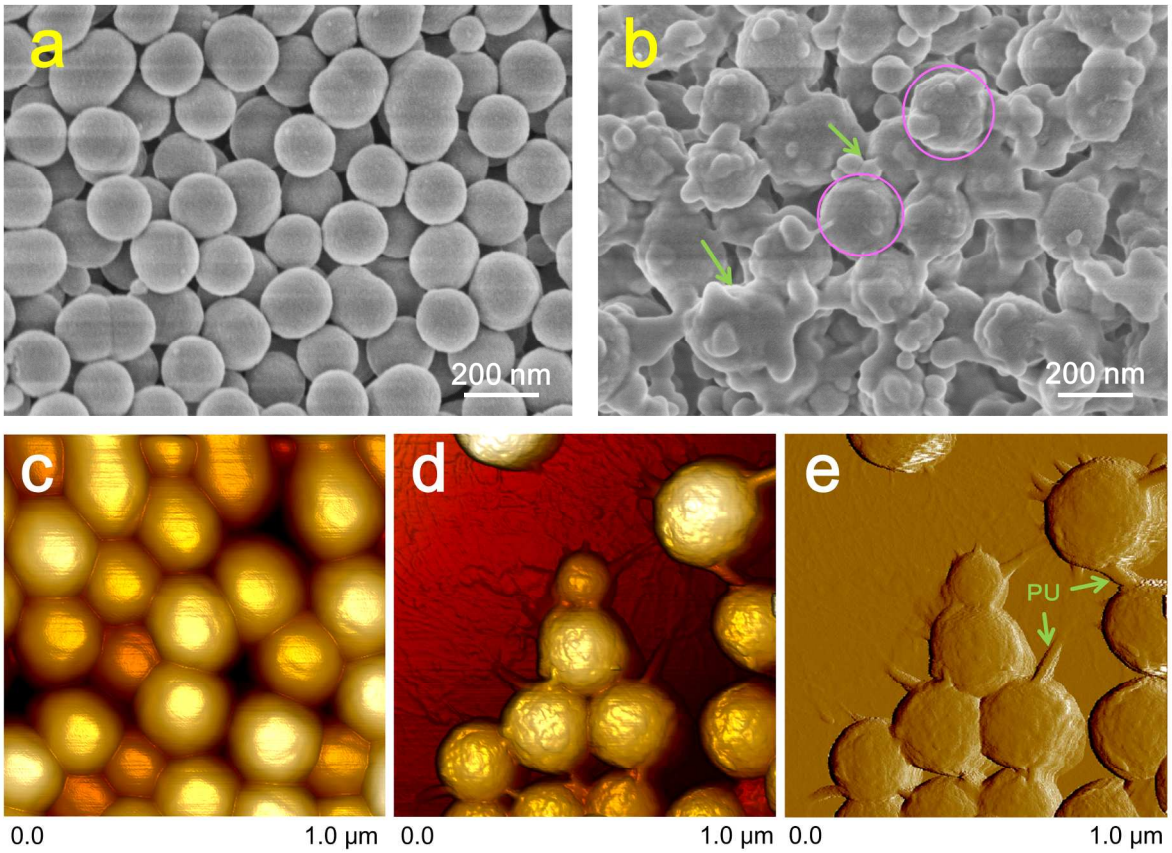

Figure 5. SEM images of (a) melanin and (b) melanin-PU nanohybrids, AFM height images of (c) melanin and (d) melanin-PU nanohybrids, AFM image of (e) melanin-PU nanohybrids was performed in a peak-force-error mode.

TEM investigation on the microstructures of PU/melanin-2 wt % nanocomposite were displayed in **Figure 6**. The shades in **Figure 6a** corresponded melanin nanoparticles and melanin were uniformly dispersed in PU with only a little aggregation. What's more, melanin were deformed into irregular shape, and displayed a black and thick interface (as shown in **Figure 6b**). The reasons for the formation of interface were ascribed to the in situ formed covalent attachment anchored stably at the interface of melanin nanoparticles and PU phase.

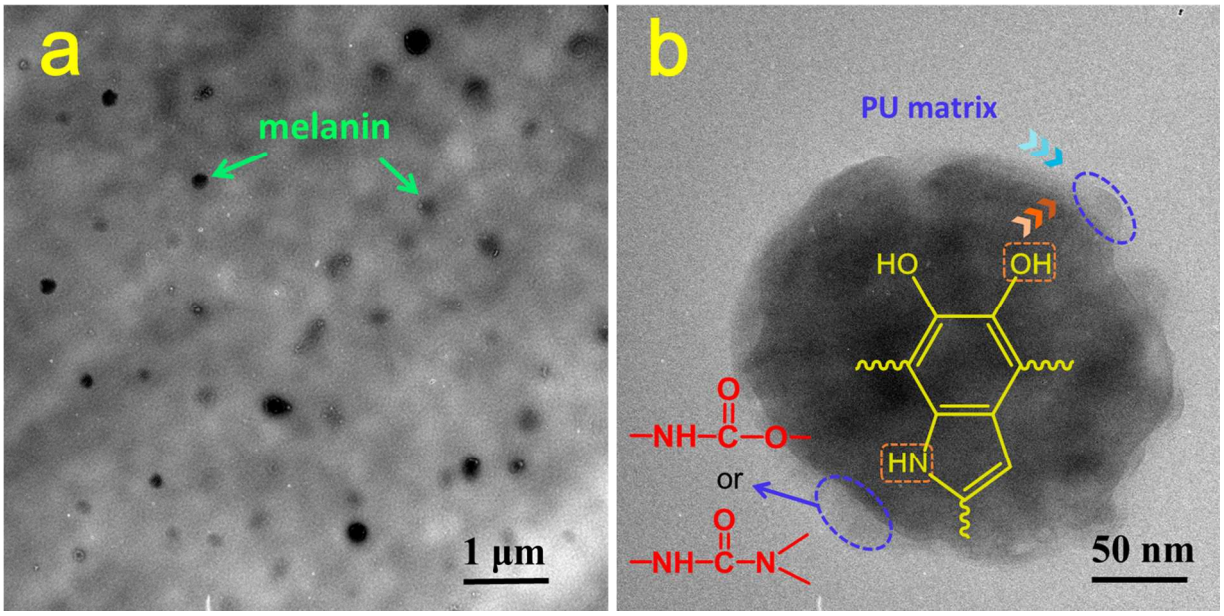

Figure 6. TEM images for PU/melanin-2 wt % nanocomposite with different magnifications.

AFM phase images of PU/melanin nanocomposites

Figure 7 showed the AFM phase images of PU and PU/melanin nanocompoaites, the bright region in the phase-angle images were representative of hard domains (high modulus) while the dark regions were corresponded to soft domains. Apparently, the phase images showed that hard domains were diluted in soft phase in pure PU and the size of hard domains were relatively small. Extensive analysis of AFM phase images revealed that as melanin was progressively added the bright areas increasingly brightened and grown in size, demonstrating that improvement of degree of phase separation. As the melanin content reached to 2 wt %, the hard domains got connected with each other. The observation suggested hard segments selectively concentrated at surface of melanin, and thus induced a more distinct phase separation. As mentioned above, the performance of PU was strongly dependent on the balance between phase separation and phase mixing. When 5 wt % melanin were incorporated, melanin could aggregate in PU matrix due to the inherent adhesive

property of melanin. As a result, the hard domains on the melanin surface subsequently aggregated, which led to grow in size and form relatively large phase separation. Therefore, nanocomposite experienced decreases in performances of PU, as discussed in the mechanical properties section.

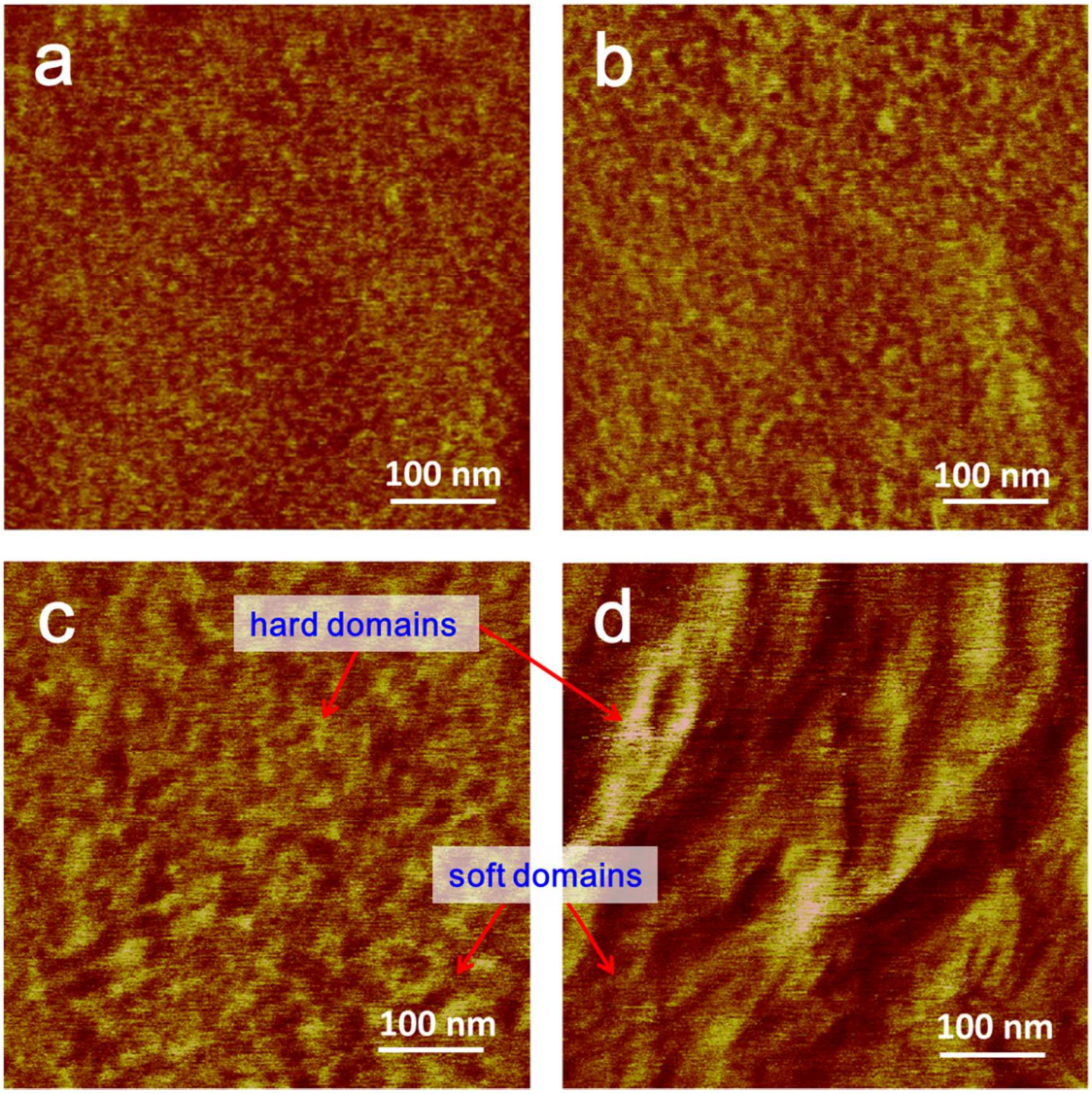

Figure 7. AFM phase images of the PU with different melanin contents: (a) 0; (b) 0.5 wt %; (c) 2 wt % and (d) 5 wt %.

Morphology of PU/melanin nanocomposites

The tensile fracture surfaces of the deformed tensile specimens were depicted in **Figure 8**. PU showed a continuous and smooth fractured surface. Compared to PU, PU/melanin-0.5 wt % nanocomposite displayed a relatively coarse and irregular fractured morphology, which indicated the changes of nanocomposite microstructure. Moreover, with the addition of 2 wt % melanin, the micrograph became significantly rough and massive local matrix deformation of PU were observed. As shown as in **Figure 8d**, clear interlocking and entanglement were found in nanocomposite, indicating a significant reinforcement of mechanical properties. Melanin induced phase separation and acted as cross-linkers which improved the cohesion force between hard segments, and suppressed the spread of cracks, hence enhancing the stiffness and toughness of nanocomposites. **Figure 9** illustrated the reinforcement mechanisms of PU reinforced with melanin nanoparticles.

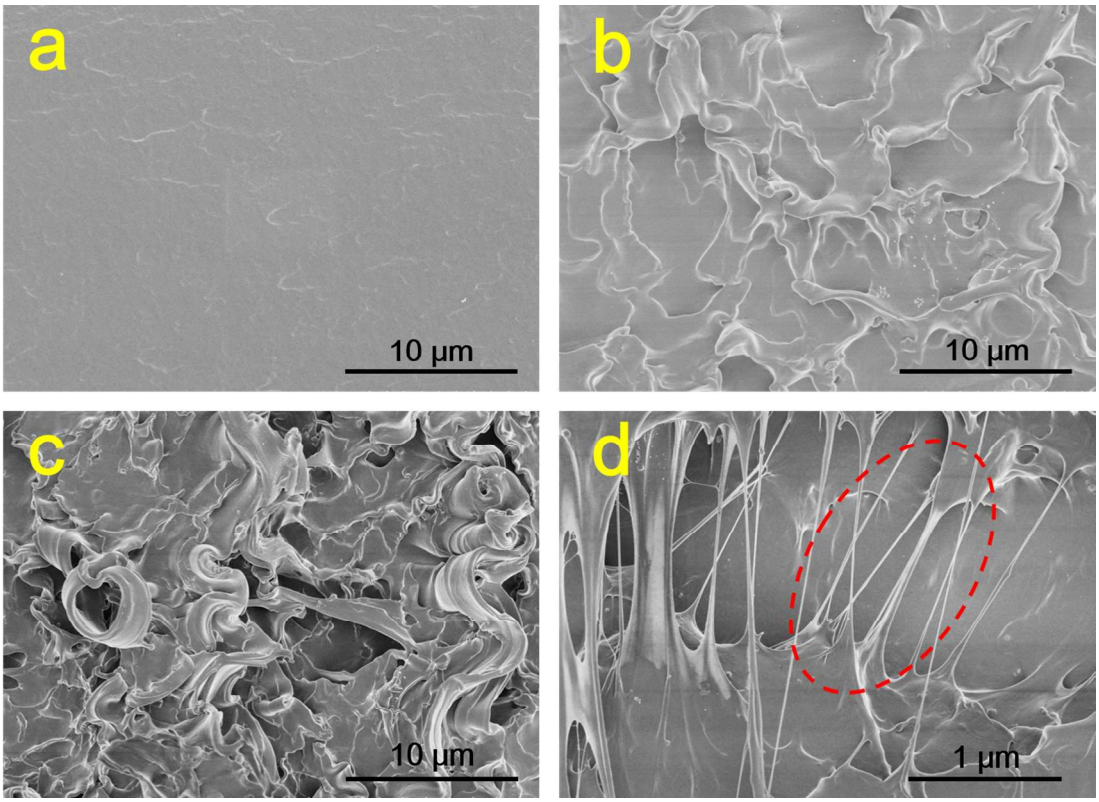

Figure 8. SEM images showing fracture surfaces of PU/melanin nanocomposites with (a) 0 wt %. (b) 0.5 wt %. (c,d) 2 wt % melanin.

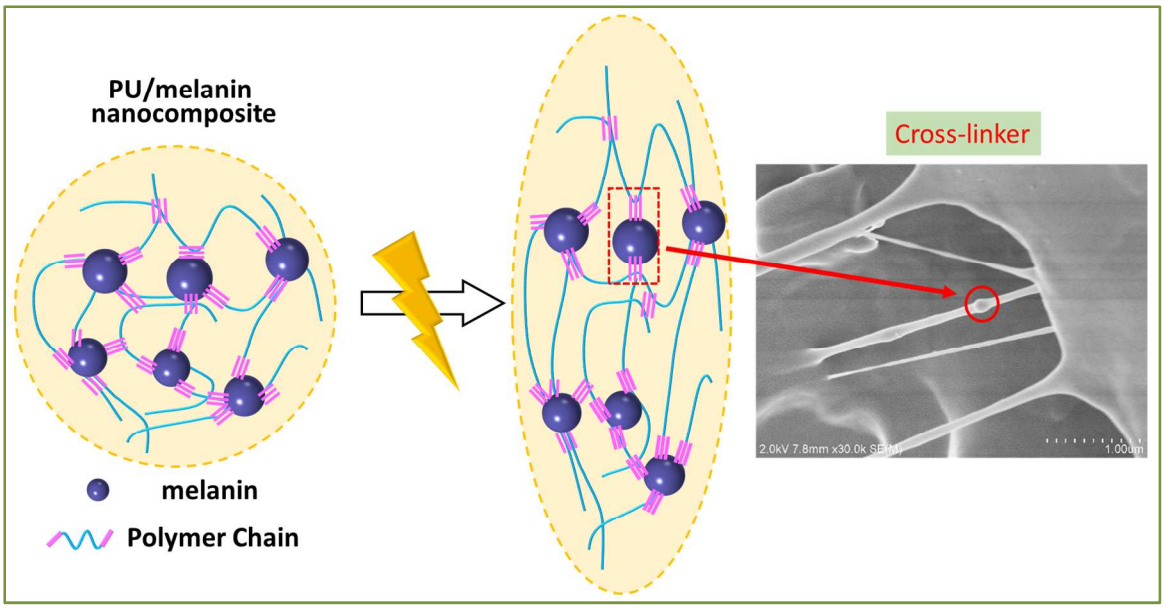

Figure 9. Enhancement mechanisms in PU/melanin nanocomposites.

Additionally, comparison of the mechanical properties of PU nanocomposites reinforced with melanin, cellulose nanocrystals (CNCs),[20] microfibrillated cellulose (MFC),[21] nanosilica (NS)[36], multiwalled carbon nanotubes (MWNTs)[37], carbon nanofibers (CNF),[38] nanoclays (NC),[39] laponite,[15] single-walled carbon nanotubes (SWNTs),[37] graphene nanosheets (GNSs)[17], and high-structured carbon black (HSCB) were shown in **Figure 10**. The other approaches for fabricating the PU nanocomposites always showed enhancement in only one kind of mechanical properties. For instance, Liff *et al.*[15] demonstrated a high strength (62 MPa) PU/Laponite nanocomposites *via* solvent exchange processing, but the ε_{max} showed a little lower. Aihua *et al.*[20] constructed high strength PU nanocmoposite with addition of CNCs. The tensile strength of

PU/CNCs-1 wt % was as high as 61.5 MPa. The dramatic increase was due to the stronger interaction between CNCs and the hard micro-domains of polyurethane. On the other hand, the strain and toughness of PU/CNCs were only 994.2% and 310 MJ/m^3, respectively. Recently, Cruz *et al*.[38] realized a high elongation PU/NS material where ε_{max} increased to 2460%, however the tensile strength was only 20 MPa. Notably, PU nanocomposites reinforced with low content of melanin exhibited a good compromise between high σ and excellent ε_{max}, outperforming PU nanocomposites improved with other nanofillers. More importantly, given that melanin is obtained either from synthetic models and many natural sources such as the cephalopoda class, plants, bacteria, etc., makes it even more significant for application.

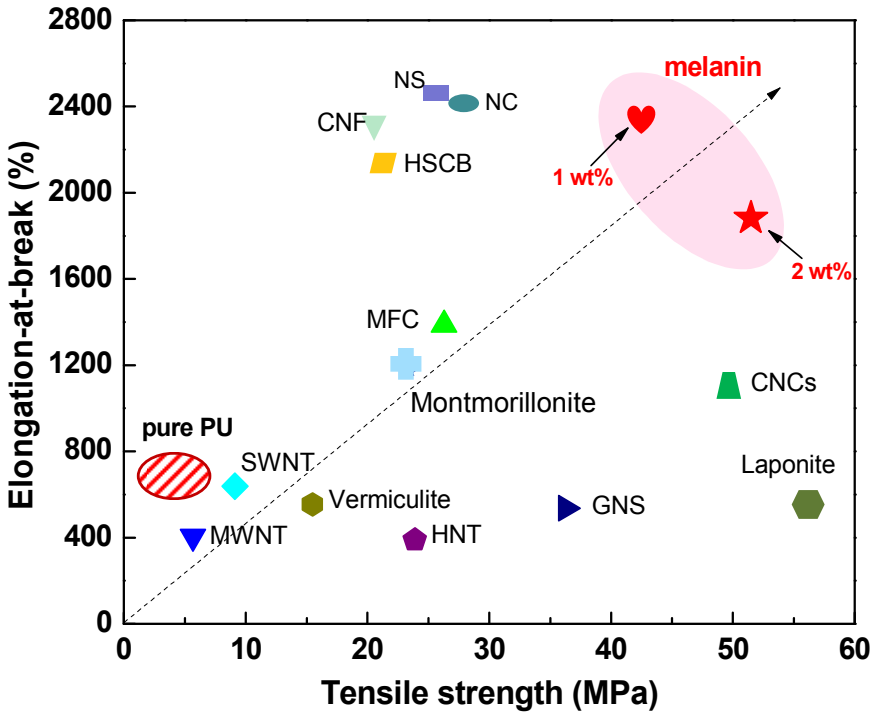

Figure 10. Comparison of σ and ε_{max} of PU/melanin nanocomposites with other PU-based materials with different nanofillers.[15, 20, 21, 34, 37, 38, 40, 41]

Rheological behavior

The storage modulus (G') and complex viscosity (η^*) of PU/melanin nanocomposites were shown in **Figure 11**. Commonly, the stronger interactions between fillers and matrix could cause a reduction of slope for plotting log G' versus log ω, and an increase of G' in low frequency region reflected the improvement in interaction strength. When 5 wt % melanin were added, the slope of log G' versus log ω in low frequency region was decreased from 0.91 to 0.12, simultaneously the slope of log η^* versus log ω decreased from -0.03 to -0.88. Obviously, nanocomposites exhibited a notable solid-like behavior in the terminal region. These phenomena indicated a slower relaxation process and an increased elasticity of the nanocomposite due to strong cohesion force between hard segments.

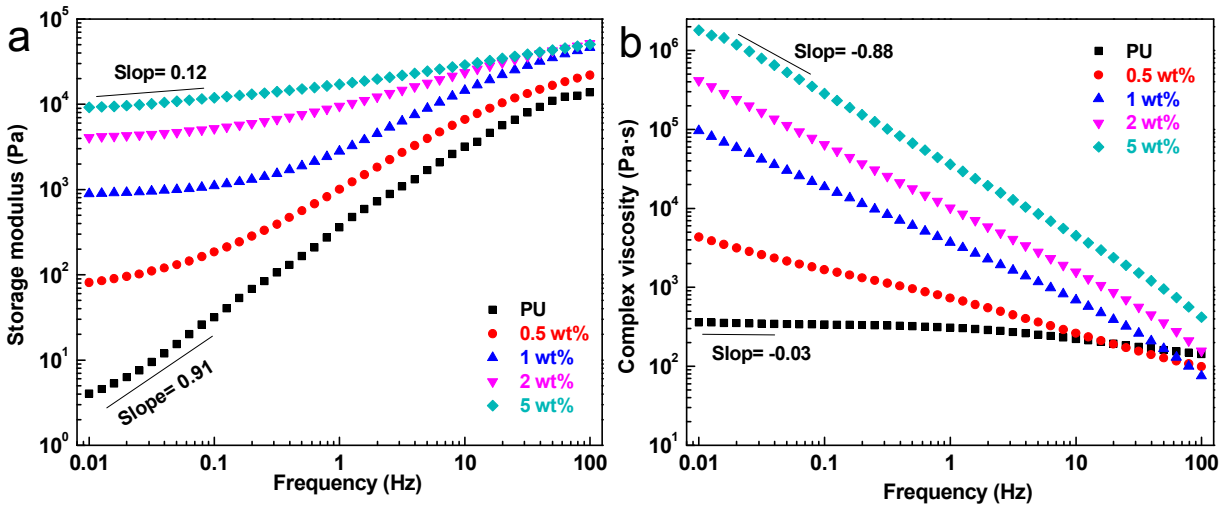

Figure 11. (a) Storage modulus (G') and (b) complex viscosity (η^*) of pure PU and PU/melanin nanocomposites as a function of frequency.

Conclusions

In this work, PU/melanin nanocomposites with high tensile strength and toughness were successfully prepared in the presence of natural melanin by *in situ* polymerization. It was observed that the tensile strength (σ), elongation-at-break (ε_{max}), Young's modulus (E_1) and toughness (W) of PU/melanin nanocomposites were enhanced simultaneously even with a small amount of melanin. With the addition of 2 wt % melanin, σ, ε_{max}, and W were increased to 51.5 MPa, 1880% and 413 MJ/m^3, respectively, which were much higher than these of PU. According to the preparation, it was found that the individualized melanin nanoparticles were specifically associated with the hard domains of PU through the chemical reaction between isocyanate of PU prepolymer and reactive groups (–OH, –NH and –COOH) of melanin nanoparticles and well dispersed in matrix, which was confirmed by micromorphology. FTIR, DSC and AFM results suggested melanin induced an improvement in phase separation. However, with further increasing melanin to 5 wt %, more hard segments concentrated on the surface of melanin, and formed a relatively large-scale phase separation, resulting in a decline in mechanical properties. On the other hand, with addition of melanin, the interaction between melanin and the hard segments was increased, leading to higher T_{gHS} enhanced. DMA results revealed that at the temperature of 20 and 60℃ the modulus of the nanocomposite (2 wt % melanin) was 600% and 830% higher than these of PU. Moreover, PU nanocomposite exhibited a notable solid-like behavior at low frequency region from rheological measurement, which suggested strong cohesion force between hard segments. The study will give us a facile method to prepare PU with high strength and toughness with addition of a little amount of melanin.

Notes

The authors declare no competing financial interest.

ACKNOWLEDGMENT

This work was supported by National Natural Science Foundation of China (51373070), the Research Project of Chinese Ministry of Education (No.113034A) and the Fundamental Research Funds for the Central Universities (JUSRP51624A).

REFERENCES

1. Liu, Z.; Luo, Y.; Bai, H.; Zhang, Q.; Fu, Q., Remarkably Enhanced Impact Toughness and Heat Resistance of poly(l-Lactide)/Thermoplastic Polyurethane Blends by Constructing Stereocomplex Crystallites in the Matrix. *Acs Sustainable Chem. Eng.* **2015,** 4, (1), 111-120.

2. Pan, Y.; Zhan, J.; Pan, H.; Wang, W.; Tang, G.; Song, L.; Yuan, H., Effect of fully bio-based coatings constructed via layer-by-layer assembly of chitosan and lignosulfonate on the thermal, flame retardant and mechanical properties of flexible polyurethane foam. *Acs Sustainable Chem. Eng.* **2015,** 4, (3), 1431-1438.

3. Wang, W.; Pan, H.; Shi, Y.; Yu, B.; Pan, Y.; Liew, K. M.; Song, L.; Hu, Y., Sandwich-like coating consisting of alternating montmorillonite and β-FeOOH for reducing the fire hazard of flexible polyurethane foam. *Acs Sustainable Chem. Eng.* **2015,** 3, (12), 3214-3223.

4. Wang, C. B.; Cooper, S. L., Morphology and properties of segmented polyether polyurethaneureas. *Macromolecules* **2002,** 16, (5), 775-786.

5. Miller, J. A.; Lin, S. B.; Hwang, K. K. S.; Wu, K. S.; Gibson, P. E.; Cooper, S. L., Properties of polyether-polyurethane block copolymers: Effects of hard segment length distribution. *Macromolecules* **1985,** 18, (1), 32-44.

6. Wiggins, M. J.; Macewan, M.; Anderson, J. M.; Hiltner, A., Effect of soft-segment chemistry on polyurethane biostability during in vitro fatigue loading. *J. Biomed. Mater. Res. A* **2004,** 68, (4), 668–683.

7. Lee, H. S.; Wang, Y. K.; Hsu, S. L., Spectroscopic analysis of phase separation behavior of model polyurethanes. *Macromolecules* **1987,** 20, (9), 2089-2095.

8. Meuse, C. W.; Yang, X.; Yang, D.; Hsu, S. L., Spectroscopic analysis of ordering and phase-separation behavior of model polyurethanes in a restricted geometry. *Macromolecules* **1992,** 25, (2), 925-932.

9. Leung, L. M.; Koberstein, J. T., DSC annealing study of microphase separation and multiple endothermic behavior in polyether-based polyurethane block copolymers. *Macromolecules* **1986,** 19, (3), 714-720.

10. Martin, D. J.; Meijs, G. F.; Gunatillake, P. A.; Mccarthy, S. J.; Renwick, G. M., The effect of average soft segment length on morphology and properties of a series of polyurethane elastomers. II. SAXS-DSC annealing study. *J. Appl. Polym. Sci.* **1997,** 64, (64), 803-817.

11. Martin, D. J.; Meijs, G. F.; Gunatillake, P. A.; Yozghatlian, S. P.; Renwick, G. M., The influence of composition ratio on the morphology of biomedical polyurethanes. *J. Appl. Polym. Sci.* **1999,** 71, (6), 937–952.

12. Gisselfält, K.; Helgee, B., Effect of Soft Segment Length and Chain Extender Structure on Phase Separation and Morphology in Poly(urethane urea)s. *Macromol. Mater. Eng.* **2003,** 288, (3), 265–271.

13. Yoshitsugu, K.; Arimitsu, U.; Masaya, K.; Akane, O.; Toshio, K.; Osami, K., Synthesis of nylon 6–clay hybrid by montmorillonite intercalated with ϵ−caprolactam. *J. Polym. Sci. Pol. Chem.* **1993,** 31, (4), 983–986.

14. Paul, P.; Kaushik, A. K.; Arruda, E. M.; Waas, A. M.; Bong Sup, S.; Jiadi, X.; Himabindu, N.; Pumplin, B. G.; Joerg, L.; Ayyalusamy, R., Ultrastrong and stiff layered polymer nanocomposites. *Science* **2007,** 318, (5847), 80-83.

15. Liff, S. M.; Kumar, N.; McKinley, G. H., High-performance elastomeric nanocomposites via solvent-exchange processing. *Nat Mater* **2007,** 6, (1), 76-83.

16. Raftopoulos, K. N.; Pielichowski, K., Segmental dynamics in hybrid polymer/POSS nanomaterials. *Prog. Polym. Sci.* **2015,** 52, 136-187.

17. Wang, X.; Hu, Y.; Song, L.; Yang, H.; Xing, W.; Lu, H., In situ polymerization of graphene nanosheets and polyurethane with enhanced mechanical and thermal properties. *J. Mater. Chem.* **2011,** 21, (21), 4222-4227.

18. Yang, L.; Si, L. P.; Toh, C. L.; Zhang, L.; Ling, H.; Chang, M.; Zhou, D.; Dong, Y.; Lu, X., Polydopamine-coated graphene as multifunctional nanofillers in polyurethane. *Rsc Adv.* **2013,** 3, (18), 6377-6385.

19. Thakur, S., Bio-based tough hyperbranched polyurethane–graphene oxide nanocomposites as advanced shape memory materials. *Rsc Adv.* **2013,** 3, (24), 9476-9482.

20. Pei, A.; Malho, J. M.; Ruokolainen, J.; Zhou, Q.; Berglund, L. A., Strong Nanocomposite Reinforcement Effects in Polyurethane Elastomer with Low Volume Fraction of Cellulose Nanocrystals. *Macromolecules* **2011,** 44, (11), 4422-4427.

21. Yao, X.; Qi, X.; He, Y.; Tan, D.; Chen, F.; Fu, Q., Simultaneous Reinforcing and Toughening of Polyurethane via Grafting on the Surface of Microfibrillated Cellulose. *Acs Appl. Mater. Interfaces* **2014,** 6, (4), 2497-2507.

22. Henriksson, M.; Henriksson, G.; Berglund, L. A.; Lindström, T., An environmentally friendly method for enzyme-assisted preparation of microfibrillated cellulose (MFC) nanofibers. *Eur. Polym. J.* **2007,** 43, (8), 3434-3441.

23. Li, J.; Wei, X.; Wang, Q.; Chen, J.; Chang, G.; Kong, L.; Su, J.; Liu, Y., Homogeneous isolation of nanocellulose from sugarcane bagasse by high pressure homogenization. *Carbohydr. Polym.* **2012,** 90, (4), 1609-13.

24. Wang, Y.; Li, T.; Ma, P.; Bai, H.; Xie, Y.; Chen, M.; Dong, W., Simultaneous Enhancements of UV-Shielding Properties and Photostability of Poly(vinyl alcohol) via Incorporation of Sepia Eumelanin. *Acs Sustainable Chem. Eng.* **2016,** 4, 2252-2258.

25. Dong, W.; Wang, Y.; Huang, C.; Xiang, S.; Ma, P.; Ni, Z.; Chen, M., Enhanced thermal stability of poly(vinyl alcohol) in presence of melanin. *J. Therm. Anal. Calori.* **2014,** 115, (2), 1661-1668.

26. Li, M. C.; Wu, Q.; Song, K.; Lee, S.; Yan, Q.; Wu, Y., Cellulose Nanoparticles: Structure–Morphology–Rheology Relationships. *Acs Sustainable Chem. Eng.* **2015,** 3, (5), 821-832.

27. Yu, H. Y.; Qin, Z. Y.; Yan, C. F.; Yao, J. M., Green Nanocomposites Based on Functionalized Cellulose Nanocrystals: A Study on the Relationship between Interfacial Interaction and Property Enhancement. *Acs Sustainable Chem. Eng.* **2014,** 2, (4), 1-16.

28. Morin, A.; Dufresne, A., Nanocomposites of Chitin Whiskers from Riftia Tubes and Poly(caprolactone). *Macromolecules* **2002,** 35, (6), 2190-2199.

29. Yeo, I.-S.; Oh, J.-E.; Jeong, L.; Lee, T. S.; Lee, S. J.; Park, W. H.; Min, B.-M., Collagen-Based Biomimetic Nanofibrous Scaffolds: Preparation and Characterization of Collagen/Silk Fibroin Bicomponent Nanofibrous Structures. *Biomacromolecules* **2008,** 9, (4), 1106-1116.

30. Meredith, P.; Sarna, T., The physical and chemical properties of eumelanin. *Pigment Cell Research* **2006,** 19, (6), 572-594.

31. Albanese, G.; Bridelli, M.; Deriu, A., Structural dynamics of melanin investigated by Rayleigh scattering of Mössbauer radiation. *Biopolymers* **1984,** 23, (8), 1481-1498.

32. Magarelli, M.; Passamonti, P.; Renieri, C., Purification, characterization and analysis of sepia melanin from commercial sepia ink (Sepia Officinalis). *Rev. CES Med. Vet. Zootec.* **2010,** 5, 18-28.

33. Wang, Y., Strong nanocomposite reinforcement effects in poly(vinyl alcohol) with melanin nanoparticles. *Rsc Adv.* **2015,** 5, (89), 72691-72698.

34. Tien, Y. I.; Wei, K. H., Hydrogen bonding and mechanical properties in segmented montmorillonite/polyurethane nanocomposites of different hard segment ratios. *Polymer* **2001,** 42, (7), 3213–3221.

35. He, Y.; Zhang, X.; Runt, J., The role of diisocyanate structure on microphase separation of solution polymerized polyureas. *Polymer* **2014,** 55, (55), 906-913.

36. Bistričić, L.; Baranović, G.; Leskovac, M.; Bajsić, E. G., Hydrogen bonding and mechanical properties of thin films of polyether-based polyurethane–silica nanocomposites. *Eur. Polym. J.* **2010,** 46, (10), 1975-1987.

37. Xia, H.; Song, M., Preparation and characterization of polyurethane-carbon nanotube composites. *Soft Matter* **2005,** 1, (5), 386-394.

38. Cruz, S. M.; Viana, J. C., Structure–Properties Relationships in Thermoplastic Polyurethane Elastomer Nanocomposites: Interactions between Polymer Phases and Nanofillers. *Macromol. Mater. Eng.* **2015,** 300, 1152-1162.

39. Maji, P. K.; Guchhait, P. K.; Bhowmick, A. K., Effect of the Microstructure of a Hyperbranched Polymer and Nanoclay Loading on the Morphology and Properties of Novel Polyurethane Nanocomposites. *Acs Appl. Mater. Interfaces* **2009,** 1, (2), 289-300.

40. Qian, Y.; Lindsay, C. I.; Macosko, C.; Stein, A., Synthesis and Properties of Vermiculite-Reinforced Polyurethane Nanocomposites. *Acs Appl. Mater. Interfaces* **2011,** 3, (9), 3709-17.

41. Ouyang, C. F.; Gong, B.; Gao, Q., Nanocomposite Reinforcement Effects in Millable Polyurethane Elastomer with Low Content of Halloysite Nanotubes. *International Conference on Material Sci. Appl.* **2015,** 68(4), 668-683.

For Table of Contents Use Only.

Superior Performance of Polyurethane Based on Melanin Nanoparticles Induced Phase Separation

Yang Wang, Ting Li, Xuefei Wang, Piming Ma, Huiyu Bai, Weifu Dong, Yi Xie, Mingqing Chen**

* Corresponding author. Weifu Dong* E-mail: wfdong@jiangnan.edu.cn.

Mingqing Chen* E-mail: mqchen@jiangnan.edu.cn

PU/melanin nanocomposites with high tensile strength and toughness are successfully prepared in the presence of natural melanin by in situ polymerization.

GRAPHICAL ABSTRACT FIGURE